



Examination on the Calculation Method for Modeling the Multi-Particle Impact Process in Cold Spraying

Shuo Yin, Xiao-fang Wang, Bao-peng Xu, and Wen-ya Li

(Submitted December 12, 2009; in revised form January 28, 2010)

In this study, a systematic examination on multi-particle impact process in cold spraying was conducted for copper material by using different methods including Lagrangian method, Eulerian method, and smoothed particle hydrodynamics (SPH) method. It is found that for the Lagrangian method, the meshing size and the element type significantly affect the resultant output. Moreover, the particle deformation behavior calculated by Eulerian method is more comparable to the experimental observation than that by Lagrangian method. Further study on the multi-particle impact process also demonstrates that Eulerian method is superior to Lagrangian method. In addition, the preliminary investigation on the mesh-free-based SPH method shows that this technique can provide a relatively reasonable result in the particle deformation behavior and the weight of the independent SPH particle exerts limited effects on the resultant output. Furthermore, owing to the meshfree feature and the appropriate solution to the contact interface, SPH method can also be employed to simulate the multi-particle impact process in cold spraying.

Keywords cold spraying (CS), copper particle, Eulerian method, multi-particle impact, numerical simulation, smoothed particle hydrodynamics (SPH) method

1. Introduction

Cold spraying (CS) is a new coating technology based on aerodynamics and high-speed impact dynamics. Differing from that of the conventional thermal spraying, the deposition process of CS relies purely on kinetic energy rather than the combination of thermal and kinetic energies of spray particles. In this process, spray particles (typically $<50\text{ }\mu\text{m}$) are accelerated to a high velocity ranging from 300 to 1200 m/s by the high speed gas flow from a De Laval nozzle (Ref 1). It has been widely accepted that there exists a material-dependent critical velocity, above which particles can adhere to the substrate through the intensive plastic deformation at a temperature well below the melting point of spray material and thus a coating can be formed (Ref 2, 3). The relatively low particle temperature makes the formation of oxygen-free

metallic coatings to be realized, which can ensure the powder feedstock to retain the original properties. Therefore, CS has been drawing more and more attention as a result of its unique advantages. However, there still exist some crucial concerns which are not well understood yet, including the bonding mechanism and actual deformation behavior.

As for the bonding mechanism of CS particles, the most prevailing hypothesis is that plastic deformation may disrupt thin surface films, such as oxides, and provide intimate conformal contact under high local pressure, thus permitting bonding to occur (Ref 3-5). Also, the formation of jetting at the local intensively deformed zones could be favorable for cleaning the crushed oxide films (Ref 2-6). Notwithstanding the hypothesis seems reasonable to explain some phenomena in CS, there are still some fundamental problems needing to be further studied, such as the metal jetting and shear instability at the contact interfaces. Therefore, it is of great importance to study the particle deformation behavior during the impact process in CS.

There are several studies focused on the impact and deformation behaviors of CS particles by both experiments and numerical simulations. Due to the extremely short impact time scale, it is difficult to observe the whole deformation process. Only the deformed particles can be observed by microscopy. Therefore, the numerical method takes an important role in studying the particle deformation process. In some studies, a coupled thermal-mechanical/hydrodynamic (CTH) code, developed at Sandia National Laboratories (Albuquerque, NM) for modeling complex multidimensional, multi-problem that are characterized by large deformation and/or strong shocks, was used. Two explicit finite element analysis

Shuo Yin and Xiao-fang Wang, School of Energy and Power Engineering, Dalian University of Technology, Dalian 116024, Liaoning, China; **Bao-peng Xu**, Faculty of Engineering, Kingston University, London SW15 3DW, UK; and **Wen-ya Li**, Shaanxi Key Laboratory of Friction Welding Technologies, School of Materials Science and Engineering, Northwestern Polytechnical University, Xi'an 710072, Shaanxi, China. Contact e-mail: yinshuo0511@yahoo.cn.



(FEA) softwares, ABAQUS and LS-DYNA, were also always used to investigate the particle impact behavior in CS.

The reported numerical results have indicated that Lagrangian method can provide a reasonable resultant output of the deformation behavior in CS (Ref 2-15). Among these results, Assadi et al. (Ref 3) used the 2D Lagrangian model to simulate the impact process of a single copper particle upon the copper substrate. They found that the plastic strain and the temperature at the contact interface goes up steeply when the onset velocity exceeds a certain critical value. Based on this finding, they concluded that the rapid increment may indicate the occurrence of adiabatic shear instability and the onset velocity can be considered as the critical velocity (Ref 3). Following this method, some researchers further investigated the particle deformation behavior and bonding features in CS by numerical method (Ref 2, 4, 8). However, most of these studies resorted to copper as standard material to describe high-strain-rate deformation, which may not represent all cases. Bae et al. (Ref 9) gave a systematical examination on the particle/substrate impact behavior using different materials as the particle and substrate. Based on the numerical results and the experimental validation, they proposed a new definition that thermal boost-up zone (TBZ) and used it to estimate the occurrence of the adiabatic shear instability. Also, they reported some different bonding features when the material properties of the particle differ from that of the substrate. Although numerical method is a useful tool to explore the bonding mechanism of CS, some studies concerning the calculation accuracy (Ref 3, 10-12) revealed that the calculated plastic strain and temperature at localized contact interfaces are much dependent on the meshing size when Lagrangian method was employed. To cope with this problem, the linear extrapolation method was developed (Ref 10) and it seems that this method can provide reasonable results in some extent. Besides, the recent studies about the calculating settings in Lagrangian method conducted by Li et al. (Ref 12, 13) provided some new findings that element type, ALE adaptive meshing, contact interaction, material damage, etc., also seriously affect the resultant output. More recently, a meshfree method called smoothed particle hydrodynamics (SPH) was used to simulate the impact process in CS, which can effectively cope with the large deformation at the contact zone and avoid the excessive distortion of elements. Although some previous studies mentioned that ALE technique also can be used to solve the large deformation problem (Ref 3, 9-13), but the applying of too much ALE technique may possibly lead to the decrease of reliability in numerical results (Ref 16). Therefore, SPH method seems more suitable in comparison to ALE technique. The preliminary numerical result of a Fe particle impacting on the Fe substrate in low-temperature high-velocity air fuel thermal spraying conducted by Yuan et al. (Ref 17) showed that SPH method is effective in solving dynamic problems of excessive distortion of elements in CS. Li et al. (Ref 18) subsequently gave a confirmation to this point through a more intensive numerical study on the SPH method.

However, notwithstanding these meaningful findings, it is noticed that most of the previous numerical studies focused on a single particle impact process. The numerical investigations on multi-particle impact process are still rare. Our preliminary study on the multi-particle impact process has demonstrated that interactions between adjacent particles significantly affect the particle deformation and the final coating formation (Ref 14). Besides, the recent numerical study on the multi-particle impact process conducted by Bae et al. (Ref 15) showed that using He as the driving gas can achieve more severe particle deformation and larger TBZ than using N₂ and also the un-preheated particle seems more possible to rebound from the substrate. Obviously, the study on the multi-particle impact is greatly important to the clarification of the coating properties as well as the bonding mechanism, thus it is worthy to pay more attention on it.

In this study, considering the importance of the calculation method which is closely relevant to the calculation accuracy and the necessity of the multi-particle impact study, the systematic examination on the calculation method including Lagrangian method, Euler method, and SPH method was conducted in order to find the suitable method for simulating the multi-particle impact process in CS.

2. Computational Descriptions

2.1 Lagrangian Method

The impact behavior of copper particles upon a copper substrate was modeled by using an explicit program LS-DYNA (Ref 19). Both 2D and 3D models were used to simulate the particle deformation behavior. For the 3D case, models were simplified as 1/4 symmetric models in order to reduce the element numbers and shorten the calculation time as shown in Fig. 1(b). The radius and height of the substrate were taken to be 4 and 6 times larger than the particle radius (10 μm). The contact process was implemented by using the erode-surface-to-surface penalty formulation available in LS-DYNA (Ref 19). The mesh was conducted using hexahedral elements. The fixed boundary condition was applied to the bottom and the free boundary condition for the others.

As for the 2D simulation, models were simplified as 1/2 symmetric models for the single impact case as shown in Fig. 1(a). The radius and height of the substrate were taken to be 8 times larger than the particle radius. The fixed boundary condition was applied to the substrate bottom and the axis of symmetry. The X-displacement of the substrate side wall was constrained and the free boundary condition for the others. For the multi-impact case, the 2D plain strain model was adopted to characterize the deformation in the center cross-section. The radius and height of the substrate were taken to be 10 times larger than the particle radius. The fixed boundary condition was applied to the substrate bottom and the X-displacement of substrate side walls was constrained. The free boundary condition was applied to the others. For both cases, the

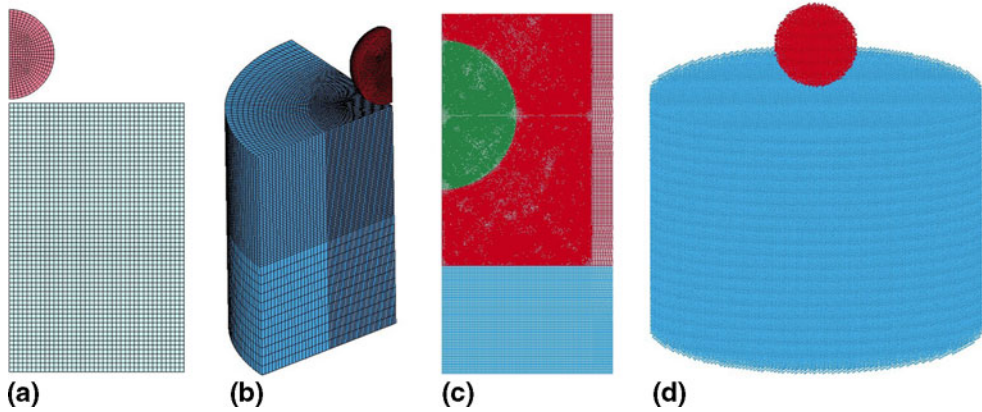


Fig. 1 Computational layouts and mesh: (a) 2D Lagrangian model, (b) 3D Lagrangian model, (c) 2D Eulerian model, and (d) 3D SPH model

contact processes were implemented by using the automatic-2d-single-surface penalty formulation available in LS-DYNA (Ref 19). The grid was conducted using quad elements. The initial velocity was chosen as 500 m/s and the initial temperature of both particle and substrate was 25 °C for all calculations in this study.

2.2 Eulerian Method

In the Eulerian simulation, the mesh was conducted by using 2D quad elements with the basic size of 0.1 μm. The model was also simplified as 1/2 symmetric model as shown in Fig. 1(c) in order to reduce the amount of elements. The radius and height of the substrate were 8 times and 6 times larger than the particle radius for the single impact case, 10 times and 6 times larger for the multi-impact case. The surrounding space where the material must flow through was meshed with the void properties setting on them. No contact penalty formulation needs to be defined, because the contact interface between different materials was estimated by calculating volume fraction of different materials in a single element. A fixed boundary condition was applied to the bottom and the axis of symmetry with the free boundary condition for the others.

2.3 SPH Method

The foundation of SPH is the interpolation theory. The conservation laws of continuum fluid dynamics are transformed into integral equations by using an interpolation function. The *kernel approximation* of a function $f(r')$ at a certain position can be obtained by using smoothing kernels, W , and then integrating over the computational domain (Ref 20, 21):

$$f(r) = \int f(r')W(r - r', h)dr' \quad (\text{Eq 1})$$

where W is a weighting function with support scale h , which satisfies the normalization condition:

$$\int W(r - r', h)dr' = 1 \quad (\text{Eq 2})$$

the Delta function property that is observed when smoothing length approaches zero,

$$\lim_{h \rightarrow 0} W(r - r', h) = \delta(r - r') \quad (\text{Eq 3})$$

There are many possible choices of kernel functions. In order to reduce the number of particle interactions and thus code efficiency, the frequently used third-order B-spline function in 3d-dimensional space was chosen as kernel function. If we define R as the relative distance between points r and r' , $R = |r - r'|/h$, then the B-spline function has the following form:

$$W(R, h) = \frac{1}{N(\delta)h^3} \begin{cases} 1 - \frac{3}{2}R^2 + \frac{3}{4}R^3 & |R| \leq 1 \\ \frac{1}{4}(2 - R)^3 & 1 < |R| \leq 2 \\ 0 & 2 < |R| \end{cases} \quad (\text{Eq 4})$$

where the normalization factor $N(\delta) = \{3/2, 7/10\pi, \pi, 31/70\pi^2, 31/5\pi^2\}$ for $\delta = 1, \dots, 5$.

The SPH momentum equation used for the fluid flow is (Ref 19):

$$\frac{dv_a}{dt} = g - \sum_b m_b \left[\left(\frac{p_a}{\rho_a^2} + \frac{p_b}{\rho_b^2} \right) - \frac{\xi}{\rho_a \rho_b} \frac{4\mu_a \mu_b}{(\mu_a + \mu_b)} \frac{v_{ab} r_{ab}}{r_{ab}^2 + \eta^2} \right] \times \nabla_a W_{ab} \quad (\text{Eq 5})$$

where p_a, ρ_a, μ_a and v_a are pressure, density, viscosity, and velocity of particle a , respectively. p_b, ρ_b, μ_b, m_b , and v_b are pressure, density, viscosity, mass, and velocity of particle b , respectively. We denote the position vector from particle b to particle a by $r_{ab} = r_a - r_b$ and let $W_{ab} = W(r_{ab}, h)$ be the interpolation kernel with smoothing length h evaluated for the distance $|r_{ab}|$. $v_{ab} = v_a - v_b$, ξ is a factor associated with the viscous term, η is a parameter used to smooth out the singularity at $r_{ab} = 0$, and g is the gravity vector.

The whole 3D SPH models were employed in this study as shown in Fig. 1(d). The radius and height of the substrate were taken as 5 times and 6 times larger than the particle radius for the single impact case, 8 times larger for the multi-impact case. The number of the independent SPH particles varied according to different cases.

The contact boundary condition does not need any special treatments in the SPH method. The contact process between the particle and the substrate is calculated through detecting the condition of the geometric proximity between a pair of SPH particles. If meeting the condition, this pair of SPH particles can be considered as contact and thus interact with each other following the compatibility boundary requirements.

2.4 Material Model

As for the material model, both the particles and the substrate were described as a Johnson and Cook plasticity model which accounts for strain and strain rate hardening, as well as thermal softening. The stresses were expressed according to the Von Mises plasticity model. The yield stress (σ_y) of this material is expressed as follows (Ref 19, 22):

$$\sigma_y = [A + B(\varepsilon_e^p)^N][1 + C \ln \dot{\varepsilon}^*][1 - (T^*)^M] \quad (\text{Eq 6})$$

where A , B , N , C , and M are material-related constants, ε_e^p is the effective plastic strain, $\dot{\varepsilon}^*$ is the effective plastic

Table 1 Material properties of copper used in simulations

Density, kg/m ³	8960
Heat capacity, J/kg · K	383
Thermal conductivity, W/m · K	386
Young's modulus, GPa	124
Poisson's ratio	0.34
A , MPa	90
B , MPa	292
N	0.31
C	0.025
M	1.09
T_m , K	1356
T_0 , K	298
Reference strain rate, 1/s	1
Gruneisen γ	2.02
Intercept of $u_s - u_p$ curve, c_0 , m/s	3940
S_1	1.49
S_2	0
S_3	0
A_0	0.47

strain rate normalized with respect to a reference strain rate. T^* is a non-dimensional temperature defined as:

$$T^* = \frac{T - T_0}{T_m - T_0} \quad (\text{Eq 7})$$

where T_m is the melting temperature and T_0 is a reference temperature. A linear Mie-Gruneisen equation of state (EOS) was employed for the elastic behavior of copper. The detailed information about Gruneisen equation can be found in Ref 17, 19. The mechanical and thermal properties were assumed to be isotropic. Copper was chosen as the particle and substrate materials and the properties used in the simulations are listed in Table 1.

3. Results and Discussion

3.1 Examination on the Lagrangian Method for Multi-Particle Impact Process

In previous studies, Lagrangian method has been widely adopted to study the deformation behavior in CS as summarized above. In this study, the more intensive examination on Lagrangian method was conducted. Figure 2 shows contours of the effective plastic strain of a single particle impacting on the substrate with different meshing sizes modeled by Lagrangian method. It is clear that the meshing size significantly affects the particle deformation. With decreasing the meshing size from 2.0 to 0.5 μm , the effective plastic strain at the contact interface increases gradually and the metal jetting at the surrounding zone becomes more and more prominent. In fact, for Lagrangian method, previous study (Ref 10, 12) has reported that the finer the mesh is, the more precise the resultant output could be. However, using fine grid also brings some serious problems including the increase in the calculating time and the abnormal termination abort of the program. Figure 3 presents the contour of the effective plastic strain at the interfacial region of a single particle with the meshing size of 0.1 μm modeled by Lagrangian method. Although such meshing size theoretically can provide the more accurate deformation behavior, the excessive distortion of the Lagrangian grid

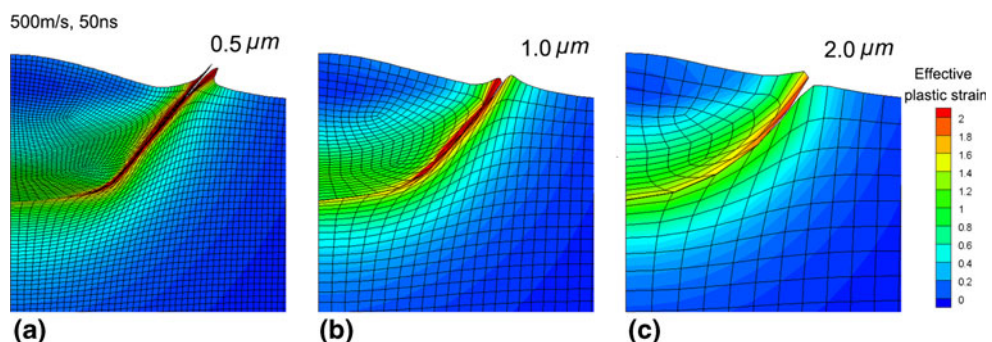


Fig. 2 Contours of the effective plastic strain of a single particle impacting on the substrate modeled by Lagrangian method with different meshing sizes: (a) 0.5 μm , (b) 1.0 μm , and (c) 2.0 μm

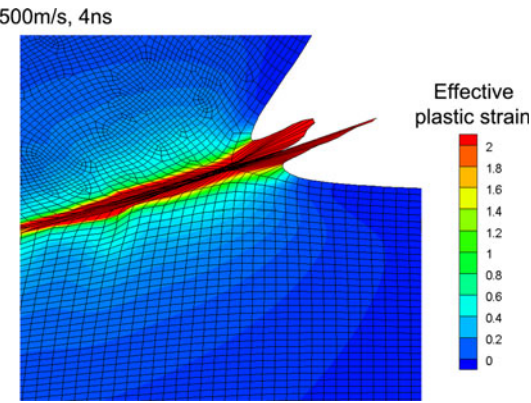


Fig. 3 Contours of the effective plastic strain at the contact interface for the particle with the meshing size of $0.1 \mu\text{m}$ modeled by Lagrangian method. Note that program terminates at 4 ns after impacting

results in the abnormal termination of the program at 4 ns after impacting.

Most of the previous studies focused on the effect of 2D meshing size on resultant outputs (Ref 10-12). Only few studies concerned about the 3D Lagrangian model (Ref 13). Figure 4 compares the deformation and the distribution of the effective plastic strain between the 3D model and the 2D model. It is obvious that the deformation characteristic and the plastic strain distribution calculated by the 3D model are similar to that by the 2D model. However, it is noticeable that there still exist some significant differences between these two simulated results. For the 3D case, the metal jetting at the surrounding region of the particle is not evident and extends much weaker than that of the substrate. While the 2D result showed a relatively obvious metal jetting at the surrounding of the particle. Furthermore, it also can be found that the effective plastic strain at the contact interface for the 3D model is smaller than that for the 2D model. The reason for these discrepancies may be linked to the fact that the 3D solid element with 8 nodes and 48 DOFs could yield more uniform deformation compared to the 2D shell element which only has 4 nodes and 6 DOFs. In addition, according to the changing tendency of the 2D models as shown in Fig. 2, it also can be deduced that if the meshing size of the 3D solid element is refined to the sufficiently small scale, the metal jetting may also be formed.

In order to obtain an insight into the effect of meshing size and element type on the resultant output, Fig. 5 shows the temporal development of the maximum effective plastic strain with different meshing sizes and mesh types modeled by Lagrangian method. For 2D models, the steep increment of the maximum effective plastic strain at certain time can be clearly observed for the meshing sizes of 0.5 and 1.0 μm . Assadi et al. (Ref 3) pointed out that this steep increase can be related to the adiabatic shear instability at the contact interface during the bonding process. However, in this study, it can be noticed that when the meshing size is increased to 2.0 μm no sharp increase is found at any time, which means Assadi's

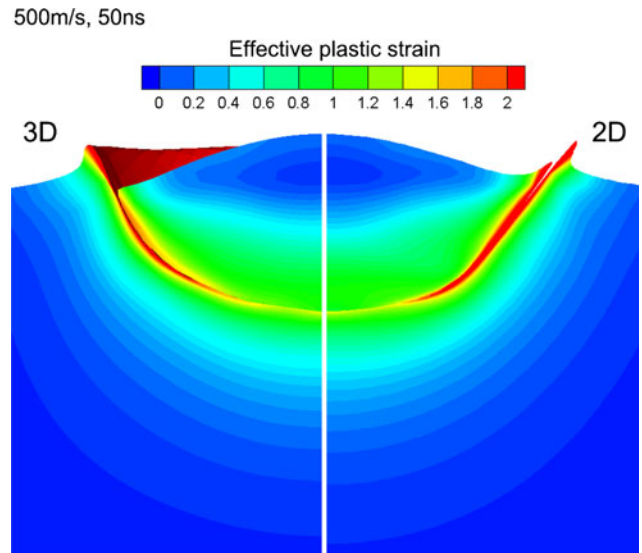


Fig. 4 Contours of the effective plastic strain of a single particle impacting on the substrate calculated by 3D model (left side) and 2D model (right side)

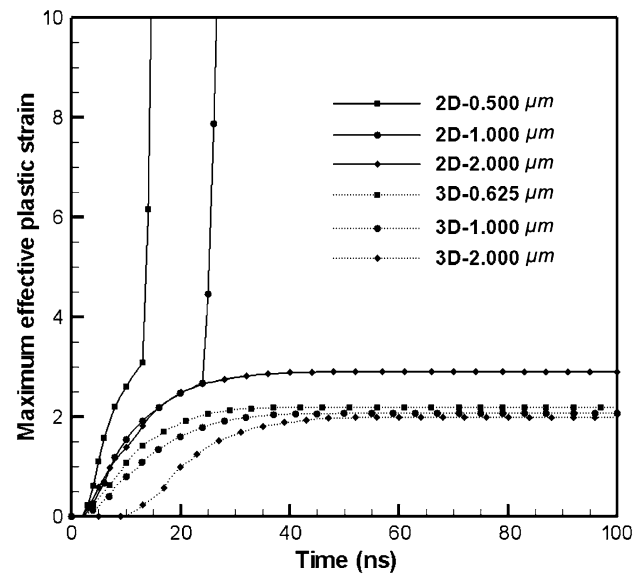


Fig. 5 Simulated temporal development of the maximum effective plastic strain modeled by Lagrangian method with different meshing sizes and different element types

method for estimating the occurrence of the shear instability may need to take the meshing size into consideration. Only for the particle with sufficiently fine meshing size, the steep increase of the maximum effective plastic strain can occur. Actually, to eliminate the effect of meshing size on numerical output, the linear extrapolation method has been used in a previous study (Ref 10). It has been recognized that this method can provide reasonable results in some extent. Moreover, it can be found that from the 3D results, there is a gradual increment in the

maximum effective plastic strain from 0 ns to around 30 ns without any sudden increase, which indicates that Assadi's estimation method for the 3D model may demand much finer mesh than the 2D model. Furthermore, it also can be seen that with refining the meshing size, the maximum effective plastic strain rises gradually. The reason for this also can be attributed to the different quantities of the nodes and DOFs for 2D shell element and 3D solid element.

The calculation of multi-particle impact process is of great importance to the clarification of the bonding mechanism as well as the in-depth analysis of coating properties in CS. Lagrangian method is firstly employed to simulate the multi-particle impact process. Figure 6 shows contours of the effective plastic strain of multi-particle impacting on the substrate. As can be seen from Fig. 6(a), prior deposited particles are tamped to irregular shapes by further impact of subsequent incident particles, while particles at the top layer deform to the lens-shape like a

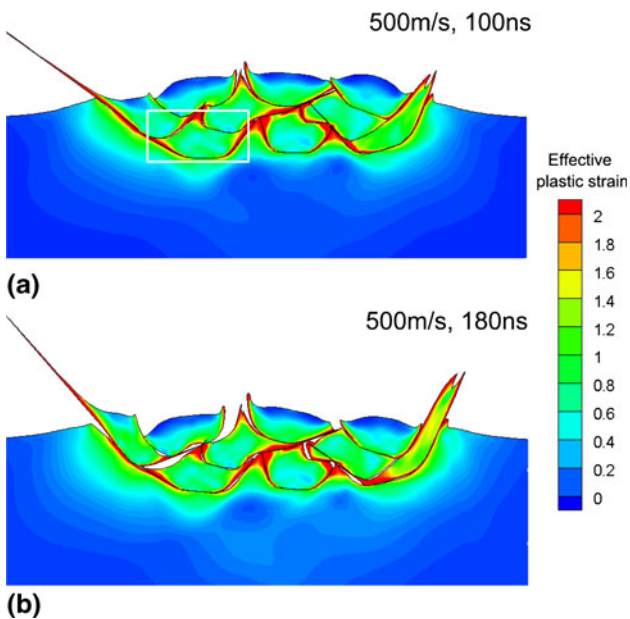


Fig. 6 Contours of the effective plastic strain of multi-particle impacting on the substrate at 100 and 180 ns modeled by Lagrangian method

single particle does. Moreover, besides the high plastic strain between the foremost deposited particles and the substrate, the relatively high plastic strain also can be found at the contact zones between adjacent particles inside the coating, which probably means the occurrence of bonding. For comparison, Fig. 7 shows the typical microstructure of cold sprayed copper coating (Ref 23). The driving gas was N₂ with the inlet pressure of 2.0 MPa and the inlet temperature of 150 °C. The substrate was located at the distance of 15 mm away from the nozzle exit. According to the experimental observation, the particle deformation inside the coating is much similar to the simulated result, especially the particle marked by the white square. However, from Fig. 6(b), it can be found that particles separate with each other at 180 ns with the generation of some gaps inside the coating. The reason for this phenomenon can be attributed to the fact that meshes attached to different materials could not be merged into integration because the Lagrangian grid node is attached on the material. Therefore, when particles complete the deformation process, the rebound force could detach the particle from the substrate and other adjacent particles. This fact may result in a serious problem that if the quantity of the incident particles is too large, the bottom particles which have finished the deformation process may rebound from the substrate and separate with each other before the whole impact process complete, which leads to inaccurate simulated results. However, although the LS-DYNA code cannot solve this problem properly at present, the ABAQUS code has been able to cope with it through constraining the contact surface to remain in contact during the impact process and this method has been used in the previous study (Ref 15).

3.2 Examination on the Eulerian Method for Multi-Particle Impact Process

Eulerian method is another technique which can be employed to simulate the impact process in CS. Differing from that in Lagrangian model, the material in Eulerian model flows through the grid which fixed in space and each element is allowed to contain a mixture of different materials. Therefore, the Eulerian method can completely avoid the element distortion. Figure 8 compares the contour of the effective plastic strain of a single particle impacting on the substrate calculated by Lagrangian

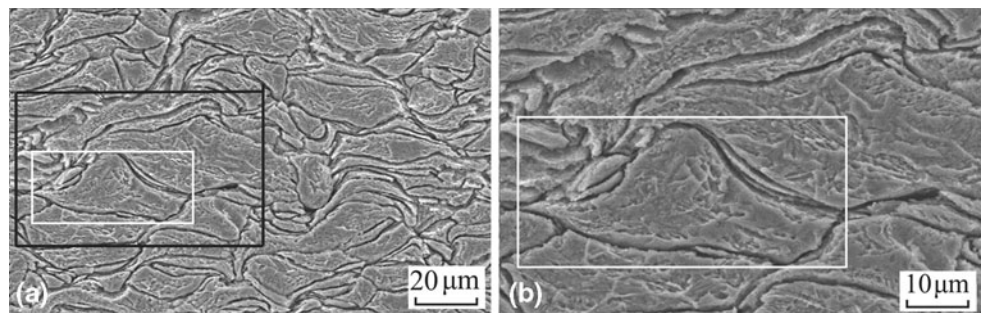


Fig. 7 Typical microstructure of cold sprayed copper coating (etched) (Ref 8)

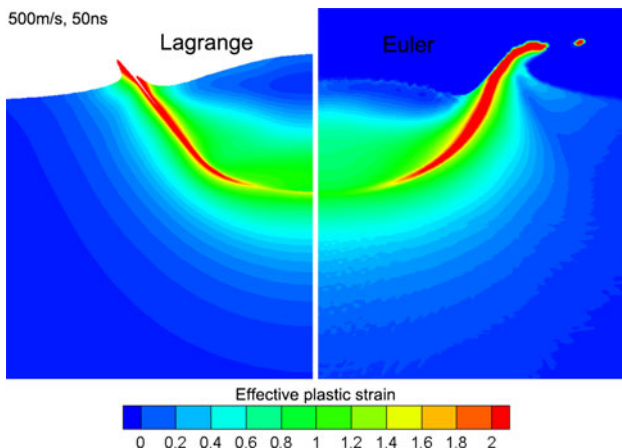


Fig. 8 Contours of the effective plastic strain of a single particle impacting on the substrate calculated by Lagrangian method (left side) and Eulerian method (right side)

method to that by Eulerian method. Obviously, the Eulerian model provides a similar particle deformation and plastic strain distribution to that of the Lagrangian model. However, some significant differences can also be found between these two methods, which are of great importance to the simulation of CS impact process. Firstly, the interface between the particle and the substrate in the Eulerian model is more undistinguishable, because the mesh is fixed in the space and materials could mix together in an element. This may be a weakness of Eulerian method. Secondly, for the same reason that the particle material and the substrate material can blend in one element, the original separate materials are integrated by the interface which was estimated by calculating volume fraction of different materials in a single element. Thus, Eulerian method can ensure the bonding between the particle and the substrate at the contact interface without rebound phenomenon after impacting, which should be quite meaningful for further coating analysis. Next, the Eulerian model needs many elements to enclose the whole surrounding space where the material might flow through during the simulation, which indicates more calculation time in comparison to the Lagrangian model. Finally, the most important finding is that the particle compression ratio of the Eulerian result is smaller than that of the Lagrangian result and also the metal jetting at the surrounding zones is more intensive and smoother. Figure 9 shows the macro photograph of the center cross-section of a copper ball with the diameter of 20 mm impacting on the low carbon steel substrate conducted by Schmidt et al. (Ref 8). Previous study (Ref 10) has reported that the similarity in deformation for particles with different diameters exists and thus the experimental result could be suitable for comparing with the simulated result in this study. It is clear that the particle deformation calculated by Eulerian method is much more comparable to the experimental observation than that by Lagrangian method, especially for the metal jetting at the surrounding contact zone, which may mean that Eulerian method can give more reasonable resultant outputs.

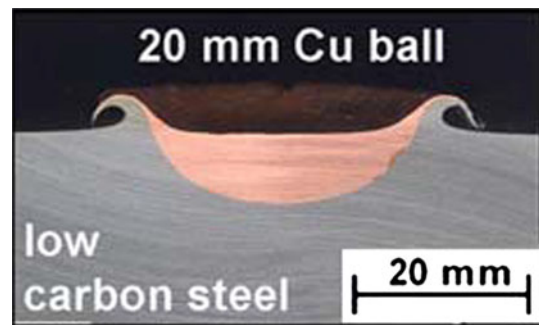


Fig. 9 Macro picture of the cross-section of a copper ball with the diameter of 20 mm impacting on the low carbon steel plate (Ref 23)

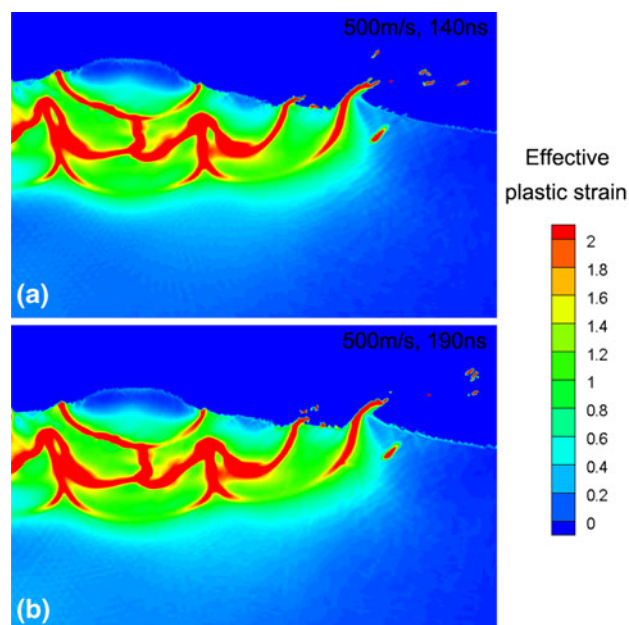


Fig. 10 Contours of the effective plastic strain of multi-particle impacting on the substrate at 100s and 180 ns modeled by Eulerian method

Figure 10 shows contours of the effective plastic strain of multi-particle impacting on the substrate modeled by Eulerian method. It is obvious that the bottom particles are tamped to irregular shapes with the significant plastic deformation present at the contact zones. Also, the top particle almost deforms independently. The deformation of the particles inside the formed thin coating is much similar to the experimental observation as shown in Fig. 7. However, the important finding here is that when the impact time reaches 190 ns at which particles have already separated with each other in the Lagrangian model result, the formed coating feature is still as the same as that in 140 ns. This fact may indicate that Eulerian method can provide not only more accurate single particle deformation, but also more precise coating feature no matter how many incident particles impact on the substrate.

Therefore, Eulerian method should be a better choice for further investigation on coating characteristic, such as the coating residual stress.

3.3 Examination on the SPH Method for Multi-Particle Impact Process

The SPH method is a non-mesh-based numerical method that can also avoid the extreme distortion of elements. The continuous material was expressed by a series of independent SPH particles which carry some important material properties. Figure 11 shows contours of the effective plastic strain of a single particle impacting on the substrate calculated by pure SPH model, the combination of Lagrangian model (substrate) and SPH model (particle) and pure Lagrangian model. For the pure SPH model, as can be seen in Fig. 11(a), SPH particles splash at the surrounding of the contact region with most of the splashed SPH particles experiencing the relatively high plastic strain like the metal jetting in Lagrangian and Eulerian simulation. As for the combination case, the particle deforms much intensively with the generation of a crater in the flat substrate, which is much more similar to the pure Lagrangian case as shown in Fig. 11(c). Moreover, the distribution of the effective plastic strain also compares fairly well with the Lagrangian result, which means the combination of Lagrangian method and SPH method can provide accurate results of the deformation in

CS. During the calculation process, some important results were also found. One is that particles do not rebound after impacting but adhere onto the substrate by using pure SPH model, which may arise from the powerful capability of the SPH method for capturing the interfacial features and handling the free surface. For the SPH method, the contact process between the particle and the substrate is calculated through detecting the condition of the geometric proximity between a pair of SPH particles. If meeting the condition, this pair of SPH particles can be considered as contact and thus interact with each other following the compatibility boundary requirements. When the incident velocity is sufficiently high, the interaction could be very intensive. SPH particles at different bodies could penetrate into each other near the interfacial surface, which results in the un-rebound of the particle. The other finding is that the combination of Lagrangian and SPH model requires the definition of the contact algorithm and sufficient numbers of independent SPH particles, otherwise the contact could not happen with the spray particle penetrating the substrate directly.

Although the SPH method is a non-mesh-based method, the weight of the independent SPH particle could be changed through setting numbers of SPH particles. Figure 12 shows the effect of SPH particle size on the spray particle deformation. The weight of each independent SPH particle is 2.61e-11g, 1.75e-11g, 1.23e-11g and 0.90e-11g. It is clearly seen that both of the particle

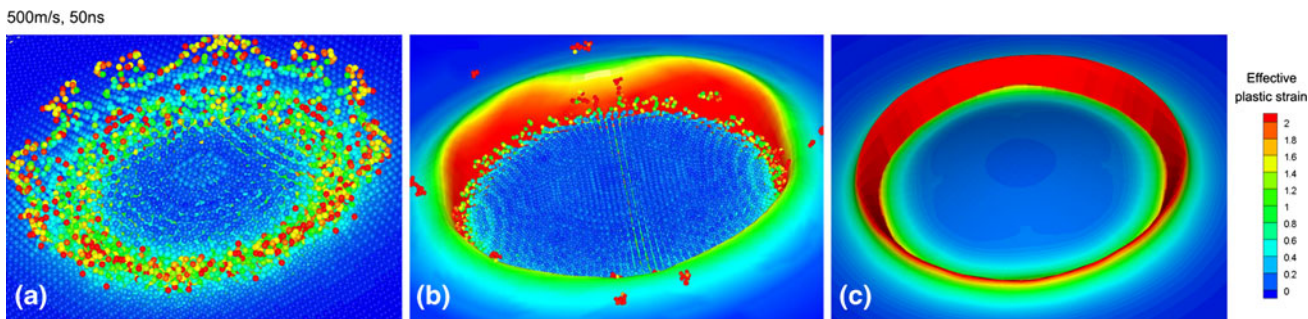


Fig. 11 Contours of the effective plastic strain of a single particle impacting on the substrate calculated by (a) pure SPH model, (b) combination of Lagrangian model (substrate) and SPH model (particle), and (c) pure Lagrangian model

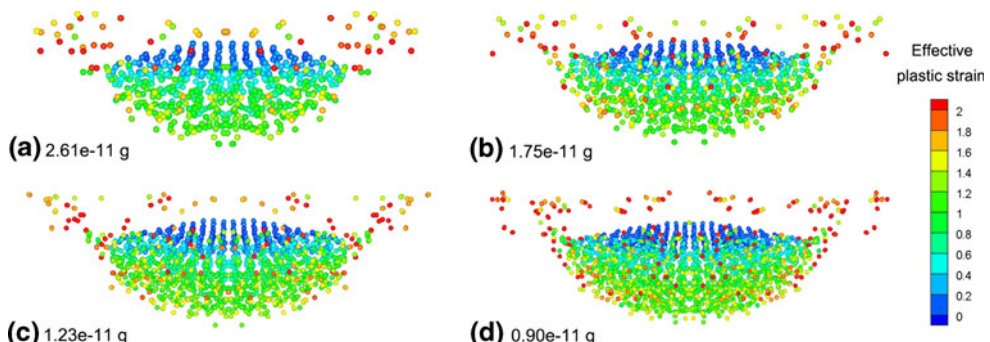


Fig. 12 Contours of the effective plastic strain of a single particle impacting on the substrate modeled by SPH method with different SPH particles sizes

deformation shape and the distribution of the effective plastic strain are much similar among different cases. The reason for this phenomenon may be linked to the mesh-free characteristic of SPH method. In order to obtain a better understanding of the effect of SPH particle size on the resultant output, the simulated temporal development of the maximum effective plastic strain modeled by SPH method is given in Fig. 13. It is obvious that for the heave SPH particle with the weight of $2.61\text{e-}11\text{ g}$, the maximum effective plastic strain is smaller than the other three cases for which the changing tendency almost has the same pattern. This fact means that the SPH particle size still affects the maximum effective plastic strain a little despite the fact that SPH method is a non-mesh-based method. In addition, it also can be found that when the weight of the SPH particle is small enough, the effect becomes indistinctive such as the case of $1.75\text{e-}11\text{ g}$, $1.23\text{e-}11\text{ g}$, and $0.90\text{e-}11\text{ g}$ in this study.

Figure 14 shows contours of the effective plastic strain and the deformation of multi-particle impacting on the substrate modeled by SPH method. It is clear that the

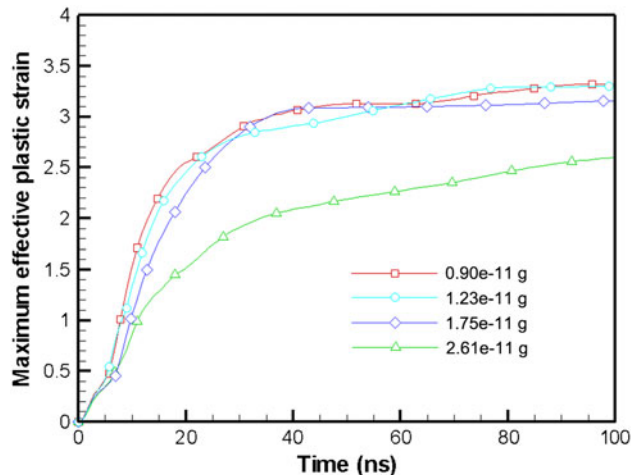


Fig. 13 Simulated temporal development of the maximum effective plastic strain modeled by SPH method with different SPH particle sizes

contact zones between different particles experience intensive plastic strain as shown in Fig. 14(a). From Fig. 14(b), it is seen that particles do not rebound from the substrate even when the impact time reaches 190 ns, which means that SPH method also can be utilized to simulate the multiple impact process regardless of the quantity of the sprayed particles. Although SPH method has some strengths such as the meshfree feature and the proper solution of the contact interface, it is not widely used yet in the field of CS because the investigation on the SPH method for simulating the impact process in CS is still in the preliminary step. Therefore, further in-depth studies on SPH method are still needed in the future research to clarify the bonding mechanism and the coating property of CS.

4. Conclusions

A comprehensive investigation on multi-particle impact process in cold spraying (CS) has been conducted for copper material by using Lagrangian method, Eulerian method, and smoothed particle hydrodynamics (SPH) method. Based on the simulated results, it is found that both the meshing size and the element type significantly influence the resultant output obtained by Lagrangian model. When Lagrangian method is used to simulate the multi-particle impact process, particles inside the coating separate with each other because the Lagrangian grid points attached to different materials could not be merged into integration. Moreover, the particle deformation behavior calculated by Eulerian method is more comparable to the experimental observation than that by Lagrangian method. Particles do not rebound from the substrate but adhere onto it. Further study on the multi-particle impact process also demonstrates that Eulerian method is superior to Lagrangian method. The bonding occurs inside the coating without any gaps and the formed coating feature compares fairly well with experiment observation. In addition, the preliminary investigation on the mesh-free-based SPH method shows that the pure SPH model and the combination of Lagrangian and SPH

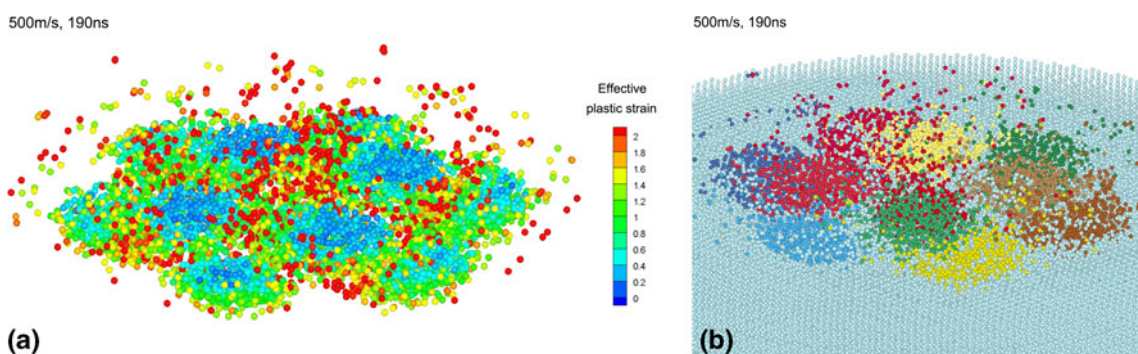


Fig. 14 Contours of (a) the effective plastic strain and (b) the deformation of multi-particle impacting on the substrate at 190 ns modeled by SPH method



model also provide a reasonable result in particle deformation behavior. Like the influence of meshing size on the resultant output in Lagrangian method, the weight of the independent SPH particle also has limited effects on the resultant output. Furthermore, owing to the meshfree feature and the appropriate solution to the contact interface, SPH method can be utilized to simulate the multi-particle impact process in CS.

Acknowledgments

The authors would like to acknowledge the financial support by National 973 Basics Science Research Program (No. 2009CB724303) and the National Natural Science Foundation of China (No. 50476075).

References

1. A. Papyrin, Cold Spray Technology, *Adv. Mater. Process.*, 2001, **159**(9), p 49-51
2. M. Grujicic, C.-L. Zhao, W.S. DeRosset, and D. Helfritch, Adiabatic Shear Instability Based Mechanism for Particles/Substrate Bonding in the Cold-Gas Dynamic-Spray Process, *Mater. Des.*, 2004, **25**(8), p 681-688
3. H. Assadi, F. Gärtnner, T. Stoltenhoff, and H. Kreye, Bonding Mechanism in Cold Gas Spraying, *Acta Mater.*, 2003, **51**(15), p 4379-4394
4. T. Schmidt, F. Gärtnner, H. Assadi, and H. Kreye, Development of a Generalized Parameter Window for Cold Spray Deposition, *Acta Mater.*, 2006, **54**(3), p 729-742
5. R.C. Dykhuizen, M.F. Smith, D.L. Gilmore, R.A. Neiser, X. Jiang, and S. Sampath, Impact of High Velocity Cold Spray Particles, *J. Therm. Spray Technol.*, 1999, **8**(4), p 559-564
6. C.-J. Li, W.-Y. Li, and H.-L. Liao, Examination of the Critical Velocity for Deposition of Particles in Cold Spraying, *J. Therm. Spray. Technol.*, 2006, **15**(2), p 212-222
7. M. Grujicic, J.R. Saylor, D.E. Beasley, W.S. DeRosset, and D. Helfritch, Computational Analysis of the Interfacial Bonding Between Feed-Powder Particles and the Substrate in the Cold-Gas Dynamic-Spray Process, *Appl. Surf. Sci.*, 2003, **219**(3-4), p 211-227
8. T. Schmidt, H. Assadi, F. Gärtnner, H. Richter, T. Stoltenhoff, H. Kreye, and T. Klassen, From Particle Acceleration to Impact and Bonding in Cold Spraying, *J. Therm. Spray Technol.*, 2009, **18**(5-6), p 794-808
9. G. Bae, Y. Xiong, S. Kumar, K. Kang, and C. Lee, General Aspects of Interface Bonding in Kinetic Sprayed Coatings, *Acta Mater.*, 2008, **56**(17), p 4858-4868
10. W.-Y. Li, H.-L. Liao, C.-J. Li, G. Li, C. Coddet, and X.-F. Wang, On High Velocity Impact of Micro-Sized Metallic Particles in Cold Spraying, *Appl. Surf. Sci.*, 2006, **253**(5), p 2852-2862
11. W.-Y. Li, H.-L. Liao, C.-J. Li, H.-S. Bang, and C. Coddet, Numerical Simulation of Deformation Behaviour of Al Particles Impacting on Al Substrate and Effect of Surface Oxide Films on Interfacial Bonding in Cold Spraying, *Appl. Surf. Sci.*, 2007, **253**(11), p 5084-5091
12. W.-Y. Li, C. Zhang, C.-J. Li, and H.-L. Liao, Modeling Aspects of High Velocity Impact of Particles in Cold Spraying by Explicit Finite Element Analysis, *J. Therm. Spray Technol.*, 2009, **18**(5-6), p 921-933
13. W.-Y. Li and W. Gao, Some Aspects on 3D Numerical Modeling of High Velocity Impact of Particles in Cold Spraying by Explicit Finite Element Analysis, *Appl. Surf. Sci.*, 2009, **255**(18), p 7878-7892
14. S. Yin, X.-F. Wang, W.-Y. Li, and B.-P. Xu, Numerical Investigation on Effects of Interactions Between Particles on Coating Formation in Cold Spraying, *J. Therm. Spray Technol.*, 2009, **18**(4), p 686-693
15. G. Bae, S. Kumar, S. Yoon, K. Kang, H. Na, H. Kim, and C. Lee, Bonding Features and Associated Mechanisms in Kinetic Sprayed Titanium Coatings, *Acta Mater.*, 2009, **57**(19), p 5654-5666
16. J.A. Zukas, *Impact Dynamics*, Wiley, New York, 1982, p 367-417
17. X.-J. Yuan, B.-L. Zha, G.-L. Hou, P.-J. Hou, L. Jiang, and H.-G. Wang, Multiscale Model on Deposition Behaviour of Agglomerate Metal Particles in a Low-Temperature High-Velocity Air Fuel Spraying Process, *J. Therm. Spray Technol.*, 2009, **18**(3), p 411-420
18. W.-Y. Li, S. Yin, and X.-F. Wang, Numerical Investigations of the Effect of Oblique Impact on Particle Deformation in Cold Spraying by the SPH Method, *Appl. Surf. Sci.* (in press). doi:[10.1016/j.apsusc.2010.01.014](https://doi.org/10.1016/j.apsusc.2010.01.014)
19. J.O. Hallquist, *LS-DYNA Theoretical Manual*, Livermore Software Technology Corporation, Livermore, CA, 1998
20. F. Colin, R. Egli, and F.-Y. Lin, Computing a Null Divergence Velocity Field Using Smoothed Particle Hydrodynamics, *J. Comput. Phys.*, 2006, **217**(2), p 680-692
21. H.H. Bui, K. Sako, and R. Fukagawa, Numerical Simulation of Soil-Water Interaction Using Smoothed Particle Hydrodynamics (SPH) Method, *J. Teruamech.*, 2007, **44**(5), p 339-346
22. G.R. Johnson and W.H. Cook, Fracture Characteristics of Three Metals Subjected to Various Strains, Strain Rates, Temperatures, and Pressures, *Int. J. Eng. Fract. Mech.*, 1985, **21**(1), p 31-48
23. W.-Y. Li, "Study on the Effect of Particle Parameters on Deposition Behavior, Microstructure Evolution and Properties in Cold Spraying," Ph.D Thesis, Xi'an Jiaotong University, China, 2005